Front. Earth Sci.
DOI 10.1007/s11707-015-0533-4

RESEARCH ARTICLE

Effects of seismic surge waves and implications for moraine-dammed lake outburst

Cui DU[1], Lingkan YAO (✉)[1,2,3], Yidan HUANG[1], Jiahong YAN[1], Subhashsagar SHAKYA[1]

1 School of Civil Engineering, Southwest Jiaotong University, Chengdu 610031, China
2 MOE Key Laboratory of High-speed Railway Engineering, Southwest Jiaotong University, Chengdu 610031, China
3 Road and Railway Engineering Research Institute, Sichuan Key Laboratory of Aseismic Engineering and Technology, Chengdu 610031, China
4 School of Civil Engineering, Henan University of Science and Technology, Luoyang 471023, China

Abstract Moraine dams usually collapse due to overtopping by the surge wave in the dammed lake, and the surge wave is most likely caused by an earthquake. The seismic water wave (SWW) is a major factor causing the dam to break in the earthquake zone. This paper focused on the SWW by model experiments with a shaking water tank under conditions of various water depths, seismic waves, and peak ground accelerations. Two empirical equations were obtained for estimating maximal wave height for the low and high frequency, respectively. Finally, we present the application of the empirical equations on Midui Glacier Lake in Tibet plateau.

Keywords seismic water wave, shaking water tank experiment, seismic wave, moraine-dammed lake outburst

1 Introduction

Moraine-dammed lakes usually threaten lives, roads, and key facilities in alpine regions (Walder and Costa, 1996; Richardson and Reynolds, 2000; Haeberli et al., 2001, 2002; Rudoy, 2002; Clague et al., 2012; Liu et al., 2013) because the dams are highly likely to collapse due to the unconsolidated soils of the moraines, leading to glacial lake outburst floods (GLOF) (Costa and Schuster, 1988; Walder and Driedger, 1995). Overtopping is one of the most common causes of dam failure (Shi et al, 2010; Emmer and Cochachin, 2013). Typically, overtopping is triggered by surge waves generated by ice or rock falls, or snow or rock avalanches (Buchroithner et al., 1982; Eisbacher and Clague, 1984; Vuichard and Zimmermann, 1987; Benn et al., 2001; Bolch et al., 2008). In alpine regions, overtopping is the main cause of moraine-dam failures due to excessive runoff during glacial retreat, snowmelt, or intensive rainfall. Destructive and erosive waves from avalanches into standing bodies of water can overtop a moraine dam, augment water flow, and cause serious erosion of the channel on top of the moraine dam. Erosion can exceed 10 m, which permits increased flow from the lake as it begins to drain (Ding and Liu, 1992; Cui et al., 2003). In particular, surge waves are sometimes caused by earthquakes and result in GLOFs (Liboutry et al., 1977; Zapata, 2002). Many glacial lakes in Tibet are located in strong earthquake regions where more than 40,000 earthquakes have been recorded since 1970 more than 3,000 of these earthquakes were greater than Ms 3. Earthquakes often produce a series of water waves that overtop the dams and cause dam breaks.

About 20 GLOFs have occurred since the 1950s on the Tibet plateau (Liu et al., 2008), and some are closely related to earthquakes. Several large debris flow events from GLOFs in Palongzangbu in the 1980s correlated to earthquakes and aftershocks (Lv et al., 1999). Generally, the maximal height of the seismic water wave (SWW) varies positively with peak ground acceleration (PGA), duration, and frequency. In 2008, the Wenchuan earthquake triggered SWW in the Zipingpu reservoir and attracted wide attention. Some model experiments on SWW were carried out using shaking table tests (Williams and Blakeborough, 2001; Shen and Lv, 2006). Sato (1967) took the seismic wave as a simple sine wave and proposed a formula for SWW height, but the results did not agree with the observed data well. More investigation is needed into SWW and its effects.

In this paper, we conduct experiments using a shaking table water tank to find the relationship between the surge wave height and the PGA, and then we use the Detrended

Received December 8, 2014; accepted May 27, 2015

E-mail: yaolk@home.swjtu.edu.cn

Cross-Correlation Analysis (DCCA) to verify the similarity of the real seismic effects and compare the experiments with the observation of SWW in Baja, California. Finally, we use the experimental results to assess the potential of GLOFs in Tibet.

2 Simulation experiment

2.1 Experimental apparatus

The shaking table consists of four parts: a platform and supporting units, the controlling system, a vibration exciter, and the hydraulic pumps (Fig. 1). The platform is 4 m × 2 m and can bear a maximum payload of 25 t. The hydraulic pump can cause the platform and supporting units to shake. The frequency of the shaking table ranges from 0.4 Hz to 15 Hz, with a corresponding maximum amplitude of ±100 mm and maximum acceleration of 1.2g (g is the gravity acceleration). The water tank is 3.76 m long, 1.76 m wide and 1.51 m high. 15 pressure sensors are installed within the tank to record the water pressure at a frequency of 50 Hz (Fig. 2). The water wave height is written as $h = P/\rho g$, with P being the water pressure and ρ the water density.

2.2 Experiment design

The experiments are designed to simulate the water waves generated by earthquakes. We consider three parameters: still water depth h_0 (cm), seismic waves, and peak seismic acceleration. At each seismic waveform and peak acceleration, the still water depth varies from 10 cm to 35 cm at an interval of 5 cm. The seismic waveforms and peak accelerations adopt the real-time records of the Wenchuan Ms 8.0 earthquake on 12 May 2008 at Wolong (Fig. 3(a)), the California earthquake Ms 7.2 on 4 April 2010 at Mexicali (Fig. 3(b)), and the synthetic Tongmai Waves that were based on rock response spectra (supplied by the institute of Crustal Dynamic China and CCCC First Highway Consultants Co., LTD, 2005). Seismic waves from the Wolong and Mexicali events represent high (> 1 Hz) and low (< 1 Hz) frequencies, respectively, while the synthetic seismic waves from Tongmai are high frequency (Fig. 4). Details of the seismic waves and corresponding PGA in experiments are shown in Table 1.

Due to the fact that the shaking tank has its own resonance frequency and that can add to the height of the water wave, a white noise is used to test the water tank's resonance frequency under different water depths.

2.3 Experiment running

In each test, the input seismic wave was created by a wave production digital control system. The vibrator then receives the signal and the shaking tank moves with the triggering seismic wave. The water surface level will change with the vibrations of the shaking tank.

More than 200 tests were carried out. The tank vibrates in a single horizontal direction, and the surge height varies with position, which is higher at the front and back of shaking tank than at the sides. This simulates when seismic waves encounter a moraine dam. Water depth data from sensors A7, A8, A14, and A15 were used to analyze the maximum water wave height, H_{max}. The water waves continue even after the seismic wave passes by. For example, in the tests with input from the Wolong seismic waves, the duration of earthquake is 80 seconds and the data recording time is about 400 seconds, as shown in Fig. 5.

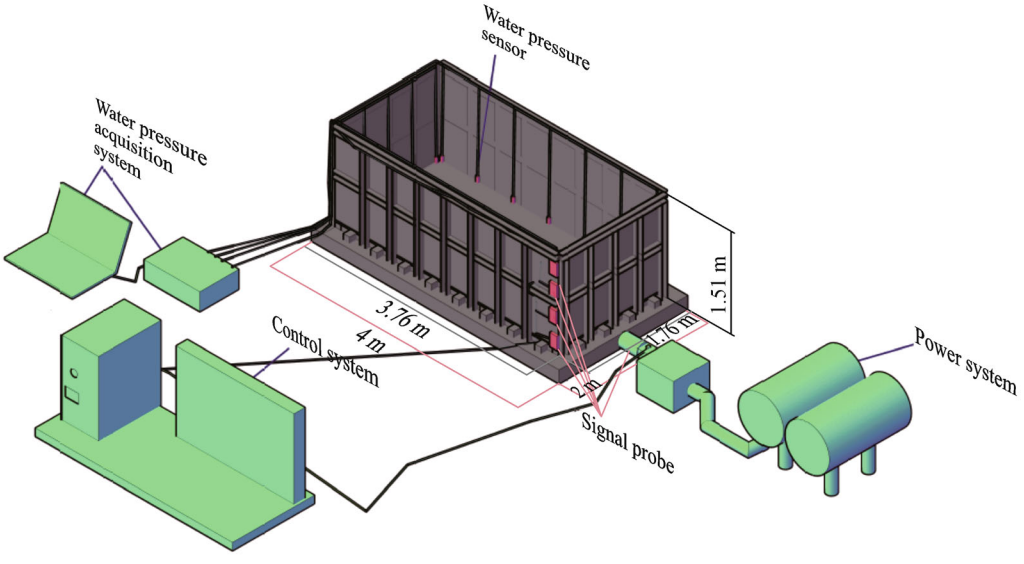

Fig. 1 Schematic diagram of the shaking table experiment.

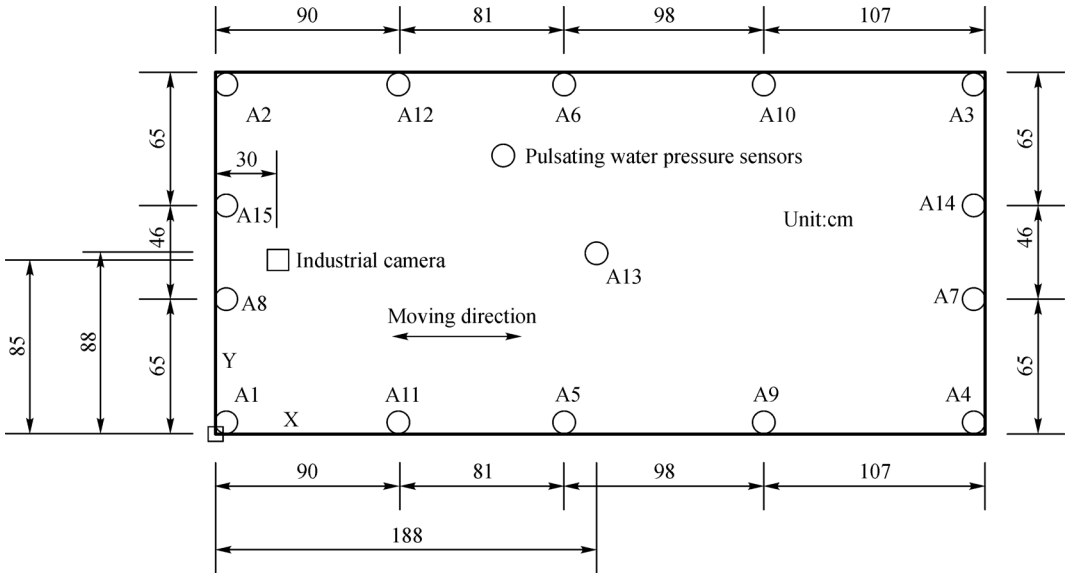

Fig. 2 Schematic diagram of pulsating water pressure sensors settings.

Table 1 Seismic wave types and PGA for the tests

Seismic waves types	Seismic acceleration/(m·s^{-2})						
Wolong wave (NS)	0.05*g*	0.1*g*	0.2*g*	0.3*g*	0.4*g*	0.5*g*	0.6*g*
Mexicali wave (NS)	0.05*g*	0.15*g*	0.2*g*	0.25*g*	0.264*g*	–	–
Tongmai wave (NS)	0.066*g*	0.25*g*	0.43*g*	–	–	–	–
White noise	0.1*g*	0.2*g*	–	–	–	–	–

"–": no available data.

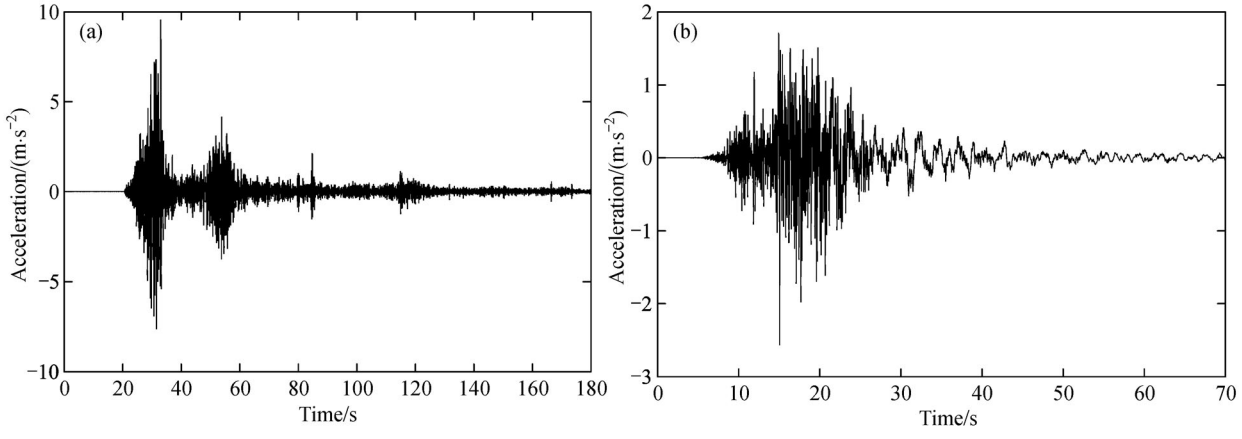

Fig. 3 The high frequency Wolong wave (a) and the low frequency Mexicali wave (b).

It is also found that H_{max} is strongly dependent positively on PGA and the water depth (Figs. 6 and 7).

2.4 Feasibility of the experiment

Before further processing the data, we use Detrended Cross-Correlation Analysis (DCCA) to assess the feasibility of the experiment.

The DCCA method is designed to investigate power-law cross correlations between different, simultaneously-recorded, non-stationary time series (Jun et al., 2006; Podobnik and Stanley, 2008; Zhou, 2008; Podobnik et al.,

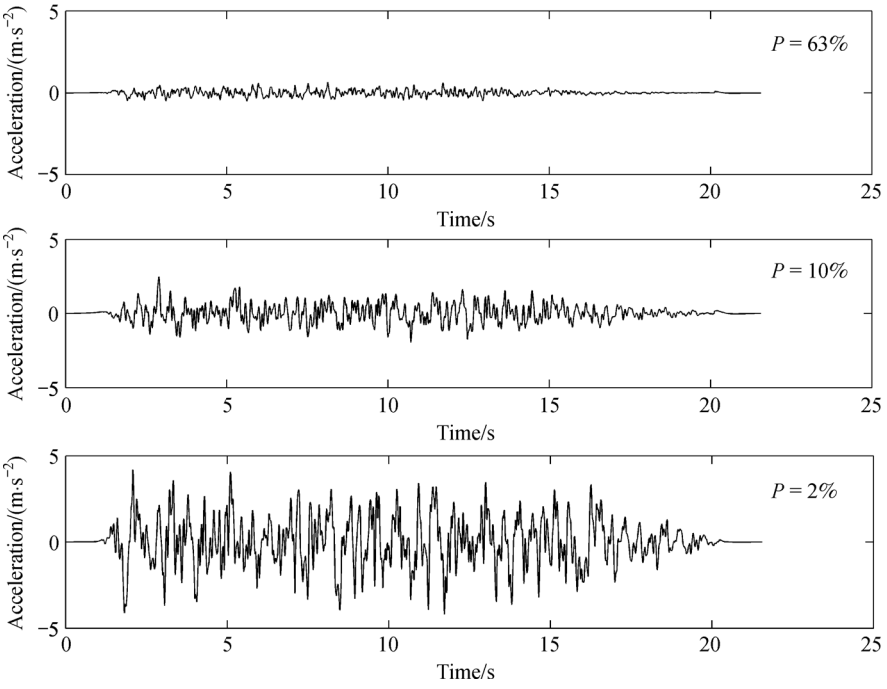

Fig. 4 Tongmai seismic wave with different exceeding probability.

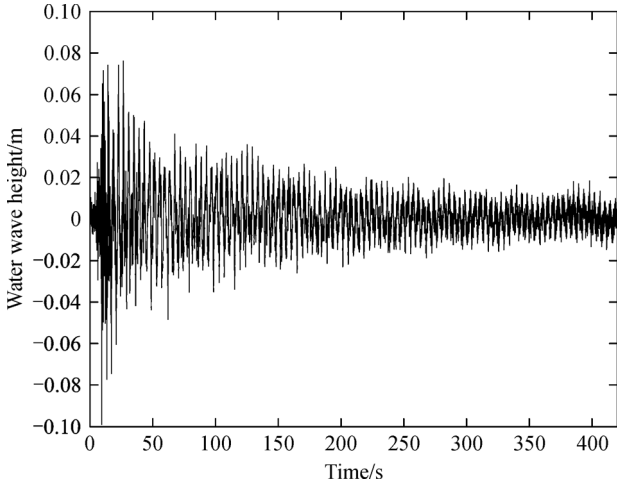

Fig. 5 The water wave curve of A7 probe with initial water depth 20 cm.

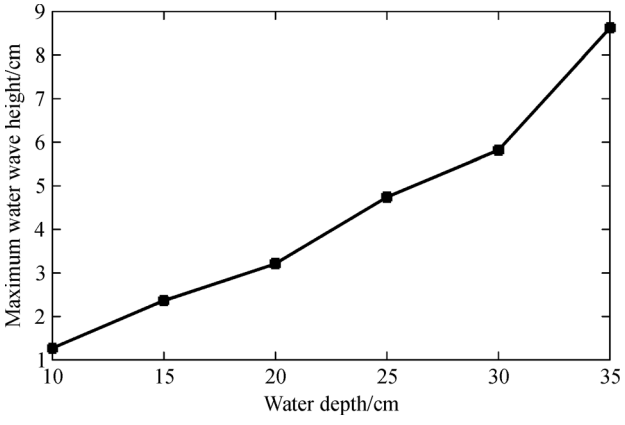

Fig. 6 Maximum water wave height increases with the initial water depth.

2009; Zebende et al., 2011). If the series is self-affine, the detrended covariance $F(n)$ satisfies the relationship $F^2(n) \sim n^d$, where n is time step length and d is the cross-correlation exponent that quantifies the long-range correlations (Zebende and Machado, 2009). The correlation is persistent (positive) when $d > 0.5$, it is anti-persistent (negative) when $d < 0.5$, and $d = 0.5$ means no cross-correlation (Wang et al., 2010).

Applying DCCA to the Mexicali seismic wave (NS) and the swimming pool water wave yields the $F(n)$ - n curve in Fig. 8. It is noted that the cross-correlations between the seismic wave and horizontal water wave are persistent within time scale $n < 4$ s (seconds), with exponent $d_1 = 1.24$. When $n > 4$ s, $d_1' = 0.48$, indicating that the cross-correlation is weak.

Figure 9 shows the $F(n)$ - n curve for the seismic wave series (NS) and the water wave series of our experiments, which is similar to Fig. 8, suggesting that the simulated water wave in the shaking tank does reflect the feature of the real water waves caused by the seismic waves.

3 Data analysis

The resonance frequency of the shaking tank was measured in several tests. Results revealed that the

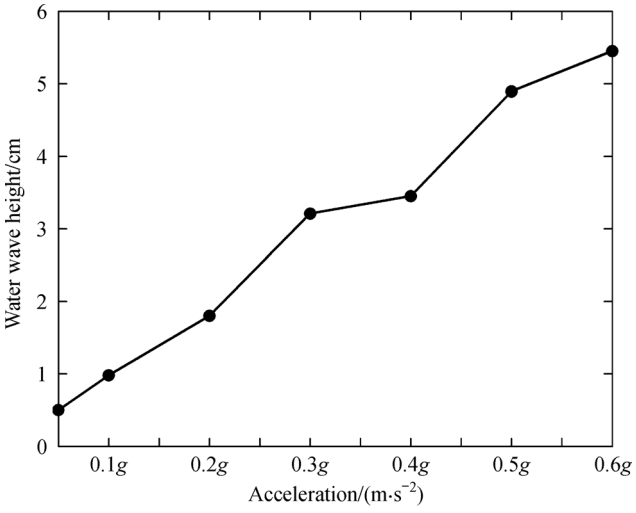

Fig. 7 Maximum water wave height increases with the PGA.

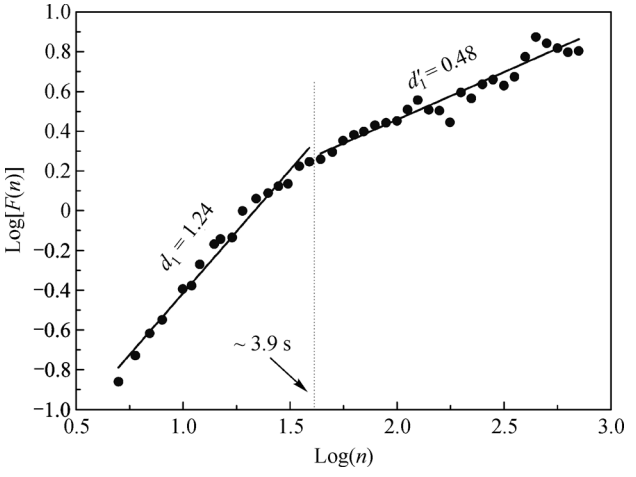

Fig. 8 Log-log plots of DCCA applied to Mexicali seismic wave series (NS) and water wave series in swimming pool.

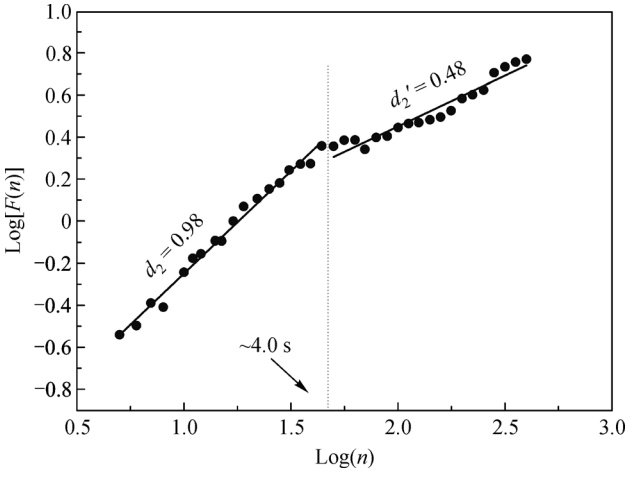

Fig. 9 Log-log plots of DCCA applied to Mexicali seismic wave series (NS) and shaking table water wave series.

resonance frequency of the shaking tank decreased with initial water level, and exceeded 60 Hz in an initial water level of 35 cm. However, the main frequency of the seismic waves in Wolong, Tongmai, and Mexicali are 1−4 Hz, 1−6 Hz, and below 1 Hz respectively. Therefore, the shaking tank will vibrate without resonance with incoming seismic waves (Wolong wave and Mexicali wave).

3.1 Relationship between water wave height and seismic acceleration

As observed above (Figs. 6 and 7), the maximum water wave height $H_{\max}$ increases monotonicly with acceleration. Figures 10 and 11 show the $H_{\max}$ increasing curves, respectively for high and low frequency of seismic waves, with different initial water depths. The experimental data are listed in Tables 2 and 3.

Dividing the measured water wave height h by the initial water depth h_0 and defining $h_L^* = h_L / h_0$ and $h_H^* = h_H / h_0$ respectively for the low and high frequency, we get the nondimensional wave height so as to remove the effect due to water depth. Then the observed data from our experiments yield the following equations:

$$h_L^* = 1.0433G^* \pm 0.05,$$

$$R^2 = 0.996, \text{ for low frequency,} \quad (1)$$

where $G^* = G/g$ is nondimensional;

And

$$h_H^* = (0.8389h_0^{*2} - 0.4094\ h_0^* + 0.4441)G \pm 0.05,$$

$$R^2 = 0.97, \text{ for high frequency,} \quad (2)$$

where $h_0^* = h_0/35$ (maximum initial water depth is 35 cm in experiments).

3.2 Comparative experiments

Similar experiments were carried out using the high frequency Tongmai waves ranging from 1 to 6 Hz. The resultant water waves agree well with Eq. (2) derived from the previous experiments, as shown in Table 4.

4 Implications for GLOF assessment

In natural conditions, seismic water waves may cause overflow of dam surfaces or move at a fast speed once the water surge surpasses the dam height, which may cause dam failure by serious scouring. For a concrete dam, the pressure is perhaps not strong enough to cause a break, such as the case of Zipingpu in the Wenchuan earthquake, where the water wave surge fluctuated more than 2 m. But for a dam formed by loose unconsolidated materials, such as a

Table 2 The maximum water wave height under input Wolong wave

PGA/(m·s^{-2})	Maximum water wave height/cm					
0.1*g*	0.7245	6.1734	1.7346	3.2551	2.2244	2.2244
0.2*g*	0.8265	7.0714	1.6428	2.5102	3.704	3.704
0.3*g*	1.2653	7.8673	3.2755	4.8265	5.9591	5.9591
0.4*g*	1.4693	3.1836	3.9183	4.602	8.0306	8.0306
0.5*g*	2.204	3.5816	5.0816	8.5714	6.7857	6.7857
0.6*g*	2.4795	5.9693	5.2244	10.7959	11.8571	11.8571

PGA: Peak ground acceleration.

Table 3 The maximum water wave height under input Mexicali wave

PGA/(m·s^{-2})	Maximum water wave height/cm					
0.05*g*	0.3877	0.6122	1.2653	1.5408	1.6122	2.1224
0.10*g*	1.1938	1.5102	1.9795	2.6326	2.2346	2.9795
0.15*g*	2.0306	2.6326	2.653	3.6632	3.7142	4.2653
0.20*g*	2.8979	4.0102	3.7755	4.5204	5.8673	5.551

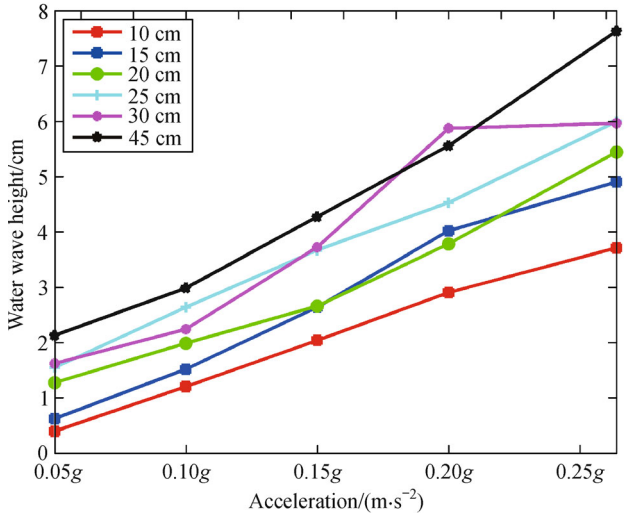

Fig. 10 Wave height varies with PGA dominated by low-frequency seismic waves (< 1 Hz).

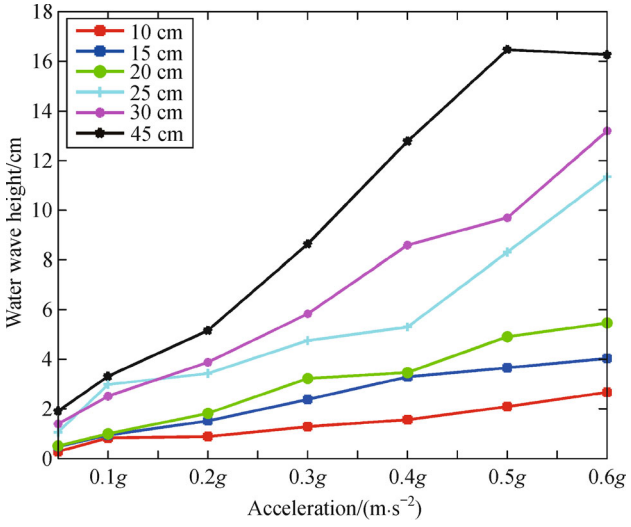

Fig. 11 Wave height varies with PGA dominated by high-frequency seismic waves (> 1 Hz).

landslide or debris flow dams, especially the moraine dams, the surge wave may result in dam failure and flooding.

For lakes full of water, a surge wave higher than 1 m may lead to disaster, such as on 21 December 1951. In Jianchuan, Yunnan, an Ms 6.3 earthquake resulted in a series of water waves in the Jianchuan Reservoir ranging from 1.3 m to 1.7 m height. Floods inundated the downstream Luying village and a vast amount of farmlands.

The Tibet Plateau is a zone with intense tectonism and strong earthquakes, where frequent earthquakes impose great threats on moraine-dammed lakes, such as the Guangxiecuo in Midui Gully (Fig. 12). The moraine there consists of granite, marble, and limestone with a compacted structure, uniform size, and weak permeability, and the lake has been increasing since 1980 due to increasing rainfall and a warmer climate, with water levels up to 17.81 m. On 15 July 1988, a block of glacial ice approximately 3.6×10^4 m^3 broke off and caused surge waves up to 3 m over the western outlet. A total of 6.01×10^6 m^3 of water poured out while about 0.97×10^6 m^3 remained. After that, the water storage has been fed by increasing rainfalls and further glacier collapses in the last years (Yang et al., 2012). At present, the water level has exceeded the outlet (Fig. 12). There is a high potentiality for dam collapse due to surge waves either by earthquake or glacier collapses.

Table 4 Comparisons between empirical calculation results and experimental results

Acceleration/(m·s^{-2})	h_f' by Eq. (2)/m	Measured h_f'/m
0.066g	0.108	0.07
0.25g	0.269	0.312
0.43g	0.426	0.501

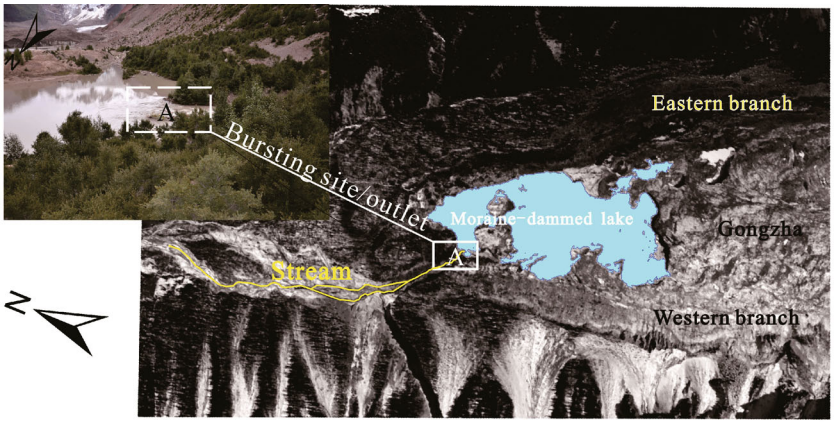

Fig. 12 Guangxiecuo moraine-dammed lake in Midui watershed of Tibet plateau.

Jiang et al. (2004) developed a formula of critical water head for moraine lake outbursts based on the theory of non-uniform sediment as:

$$H_0 = 23.4 d_{95}^{0.583} / [10^{0.833b/B} (B/b)^{0.697}], \quad (3)$$

where B is the length of moraine dam in meters, and b is the width of the rectangular outburst outlet with the same unit, d_{95} is the particle diameter over 95 percentage of the moraine materials. This glacial lake is 680 m in length, 400 m in width and with an average water depth of 10.2 m. The critical water level is 0.83 m.

We can estimate the possibility of dam failure based on the previous discussions. Considering different PGA, Table 1 indicates that, within 50 years, the exceeding probability of 0.066g, 0.25g, and 0.43g are 63%, 10%, and 2%, respectively. Accordingly, the maximal heights of the water waves calculated by Eq. (2) are 0.78 m, 1.52 m, and 2.25 m. Therefore, the Guangxiecuo is likely safe with a collapse probability of 63%. But once the PGA exceeds 0.25g, the moraine dam is highly like to collapse.

5 Discussion and conclusions

SWW may have an important role in glacial lake outbursts. The shaking tank table experiments show that the maximal height of the water wave increases with initial water level and PGA; the observed data derives two empirical relationships between the maximal height and PGA respectively for high and low frequency seismic waves.

The empirical relationships can be used to assess the outburst potentiality of dammed lakes caused by the SWW, such as indicated by the case study of the Guangxiecuo glacier lake in Tibet.

Admittedly, the present study considers only the maximal wave height, which is generally not sufficient to cause a dam break. Further studies should be focused on the interaction between wave and dam, especially the wave fluctuant pressure on dam stability, as well as the temporal effects of the seismic wave.

The relationship between the different directions of earthquake waves and the water waves using DCCA method analysis show that the NS is stronger than others. Therefore, the earthquake wave in NS direction was used only in this experiment. In future study, we will try to carry out three dimensional shaking water tank table experiments.

Acknowledgements These works were supported by the National Natural Science Foundation of China (Grant Nos. 41571004, 41172321, and 41030742), and the Southwest Jiaotong University Doctor Innovation Fund. We thank Yuncheng Zhang, Yiliang Zhou, Haiqiang Guo, and Hongzhou Ai for their work in fields.

References

Benn D I, Wiseman S, Hands K A (2001). Growth and drainage of supraglacial lakes on debrismantled Ngozumpa Glacier, Khumbu Himal, Nepal. J Glaciol, 47(159): 626–638

Bolch T, Buchroithner M F, Peters J, Baessler M, Bajracharya S (2008).

Identification of glacier motion and potentially dangerous glacial lakes in the Mt. Everest region/Nepal using spaceborne imagery. Nat Hazards Earth Syst Sci, 8(6): 1329–1340

Buchroithner M, Jentsch G, Wanivenhaus B (1982). Monitoring of recent geological events in the Khumbu area (Himalaya, Nepal) by digital processing of Landsat MSS data. Rock Mech, 15(4): 181–197

Clague J J, Huggel C, Korup O, McGuire B (2012). Climate change and hazardous processes in high mountains. Rev Asoc Geol Argent, 69 (3): 328–338

Costa J E, Schuster R L (1988). The formation and failure of natural dams. Geol Soc Am Bull, 100(7): 1054–1068

Cui P, Ma D T, Chen N S, Jiang Z X (2003). The initiation, motion and mitigation of debris flow caused by glacial lake outburst. Quaternary sciences, 23(6): 621–628 (in Chinese)

Ding Y, Liu J (1992). Glacial lake outburst flood disasters in China. Ann Glaciol, 16: 180–184

Eisbacher G H, Clague J J (1984). Destructive mass movements in high mountains: hazards and management. Geological Survey of Canada Paper, 84–16: 426

Emmer A, Cochachin A (2013). The causes and mechanisms of moraine-dammed lake failures in the Cordillera Blanca, North American Cordillera, and Himalaya. Acta Univ Carol Geogr, 48(2): 5–15

Haeberli W, Kaab A, Muhll D V, Teysseire P (2001). Prevention of outburst floods from periglacial lakes at Grubengletscher, Valais, Swiss Alps. J Glaciol, 47(156): 111–122

Haeberli W, Kaab A, Paul F, Chiarle M, Mortara G, Mazza A, Deline P, Richardson S D (2002). A surge-type movement at Ghiacciaio del Belvedere and a developing slope instability in the east face of Monte Rosa, Macugnaga, Italian Alps. Norsk Geografisk Tidsskrift-Norwegian Journal of Geography, 56(2): 104–111

Jiang Z X, Cui P, Jiang L V (2004). Critical hydrologic condition for overflow burst of Moraine Lake. Journal of Railway Engineering, 84 (4): 21–26 (in Chinese)

Jun W C, Oh G, Kim S (2006). Understanding volatility correlation behavior with a magnitude cross-correlation function. Phys Rev E Stat Nonlin Soft Matter Phys, 73(6): 066128

Liboutry L, Morales B A, Pautre A, Schneider B (1977). Glaciological problems set by the control of dangerous lakes in Cordillera Blanca, Peru, I. Historical failures of moraine dams, their causes and prevention. J Glaciol, 18(79): 255–273

Liu J J, Tang C, Cheng Z L (2013). The two main mechanisms of glacier lake outburst flood in Tibet, China. Journal of Mountain Science, 10 (2): 239–248

Liu W, Guo Q, Wang Y (2008). Temporal-spatial climate change in the last 35 years in Tibet and its geo-environmental consequence. Environmental Geology, 54(8): 1747–1754

Lv R R, Tang B X, Zhu P Y (1999). Debris Flow and Environment in Tibet. Chengdu: Chengdu Science and Technology University Press

Podobnik B, Horvatic D, Petersen A M, Stanley H E (2009). Cross-correlations between volume change and price change. Proc Natl Acad Sci USA, 106(52): 22079–22084

Podobnik B, Stanley H E (2008). Detrended cross-correlation analysis: a new method for analyzing two nonstationary time series. Phys Rev Lett, 100(8): 084102

Richardson S D, Reynolds J M (2000). An overview of glacial hazards in the Himalayas. Quat Int, 65–66(1): 31–47

Rudoy A N (2002). Glacier-dammed lakes and geological work of glacial super floods in the Late Pleistocene, Southern Siberia, Altai Mountains. Quat Int, 87(1): 119–140

Sato Q (1967). Seismic waves in reservoirs generated by earthquake. Civil engineering materials, 9: 480–482 (in Japanese)

Shen J D, Lv X L (2006). Research advances on simulating earthquake shaking tables and model test. Struct Eng, 22(6): 55–63 (in Chinese)

Shi Z M, Li J K, Lu C L, Wang Y Q, Xu Q (2010). Research status and prospect of the stability of Landslide dam. Journal of Engineering Geology, 18(5): 657–663 (in Chinese)

Vuichard D, Zimmermann M (1987). The 1985 catastrophic drainage of a moraine-dammed lake, Khumbu Himal, Nepal: cause and consequences. Mt Res Dev, 7(2): 91–110

Walder J S, Costa J E (1996). Outburst floods from glacier-dammed lakes: the effect of mode of lake drainage on flood magnitude. Earth Surf Process Landf, 21(8): 701–723

Walder J S, Driedger D L (1995). Frequent outburst floods from south Tahoma glacier, Mount Rainier, USA: relation to debris flow, meteorological origin and implications for subglacial hydrology. J Glaciol, 41(137): 1–10

Wang Y, Wei Y, Wu C (2010). Cross-correlations between Chinese A-share and B-share markets. Physica A: Statistical Mechanics and its Applications, 389(23): 5468–5478

Williams M S, Blakeborough A (2001). Laboratory testing of structures under dynamic loads: an introductory review. Philosophical transactions, 359(1786): 1651–1669

Yang R M, Zhu L P, Wang Y J, Chu D (2012). Study on the variations of lake area & volume and their effect on the occurrence of outburst of MUDUI glacier lake in southeastern Tibet. Progress in Geography, 31(9): 1133–1140 (in Chinese)

Zapata L M (2002). La dinamica glaciar en lagunas de la Cordillera Blanca. Acta Montana, 19(123): 37–60

Zebende G F, Da Silva P A, Machado Filho A (2011). Study of cross-correlation in a self-affine time series of taxi accidents. Physical A: Statistical Mechanics and its Applications, 390(9): 1677–1683

Zebende G F, Machado F (2009). Cross-correlation between time series of vehicles and passengers. Physical A: Statistical Mechanics and its Applications, 388(23): 4863–4866

Zhou W X (2008). Multifractal detrended cross-correlation analysis for two nonstationary signals. Phys Rev E Stat Nonlin Soft Matter Phys, 77(6): 066211